Surgery Open Digestive Advance 18 (2025) 100213

Contents lists available at ScienceDirect

Surgery Open Digestive Advance

journal homepage: www.elsevier.com

Original Article

Sleeve gastrectomy elicits alterations in gastric motility and morphometry in obese rats

Michael Jose Abílio de Almeida [a,*], Gustavo Serafim Rodrigues [a], Leonardo Antônio Pinto [a], Erick Guilherme Stoppa [a], Mariana Pirani Rocha Machado [a], Loyane Almeida Gama [b], Guilherme Augusto Soares [a], Rozemeire Garcia Marques [c], Madileine Francely Américo [b], José Ricardo de Arruda Miranda [a]

[a] Institute of Biosciences, Department of Biophysics and Pharmacology, São Paulo State University, UNESP, Botucatu, Brazil
[b] Institute of Biological Sciences and Health, Federal University of Mato Grosso, UFMT, Barra do Garças, Brazil
[c] Botucatu School of Medicine, Department of Surgery and Orthopedics, UNESP, Botucatu, Brazil

ARTICLE INFO

Article History:
Received 3 December 2024
Accepted 11 April 2025
Available online 4 June 2025

Keywords:
Gastric contractility
Gastric emptying
Magnetic techniques
Orocecal transit time
Sleeve gastrectomy

ABSTRACT

Background: Sleeve gastrectomy (SG) is a bariatric procedure resulting in long-term weight loss, but detailed studies on gastric contractility and gastrointestinal transit in the same subject are absent. This study aimed to evaluate the effects of SG on gastrointestinal motility in rats using alternating current biosusceptometry (ACB).
Methods: Male Wistar rats were fed with a high sugar-fat diet for 12 weeks and randomly assigned to four experimental groups: Control; Control + SG; Obese; and Obese + SG. GI motility measurements were performed using the ACB technique. Mean gastric emptying time (MGET), mean cecum arrival time (MCAT), and frequency gastric contractility were assessed. Moreover, nutritional, lipid profile, and morphometry analysis, were evaluated 30 days after surgery. Data were analyzed by ANOVA followed by post Tukey or Kruskal-Wallis test followed by Dunn's multiple comparisons test.
Results: SG significantly accelerated both MGET and MCAT compared to controls, indicating faster gastric emptying and orocecal transit. Gastric contractility was severely impaired, with reduced dominant frequency and non-stationary, non-sinusoidal waveforms observed post-SG. Morphometric analysis revealed reduced mucosal and muscularis layer thickness and increased leukocyte infiltration, indicating inflammation and tissue remodeling.
Conclusions: The excision of the gastric greater curvature in SG induced persistent dysmotility, accelerating GI transit and impairing gastric contractile function, accompanied by significant morphometric changes. These alterations may have long-term effects, underscoring the importance of extended follow-up in SG studies.

1. Introduction

The prevalence of obesity and an overweight condition is increasing globally, and comorbidities associated with obesity, such as hypertension and type 2 *diabetes mellitus,* result in increased mortality and morbidity[1]. Although strategies such as pharmacotherapy and lifestyle changes may temporarily alleviate obesity symptoms[2], bariatric surgery is the most effective approach, resulting in substantial weight loss with the remission of comorbidities[3].

Sleeve gastrectomy (SG) presents long-term effectiveness of weight loss in the treatment of morbid obesity[4], [5]. The procedure involves removing the stomach's fundus and the greater curvature, but the mechanism to achieve consistent weight loss is complex. The excised portions of the stomach play a key role in gastrointestinal (GI) function, where the fundus is responsible for receptive relaxation, and the greater curvature is the dominant site of the interstitial cells of Cajal (ICC) and responsible for producing ghrelin[6,7]. The remaining narrow sleeve is characterized by lesser distensibility and higher intraluminal pressure, resulting in early satiety[8].

GI motility comprises several processes, including gastric emptying, GI transit, contractile activity (mechanical and myoelectrical), tone, and compliance[9]. Although previous studies conducted in humans showed that SG accelerates gastric emptying and small bowel transit, few studies have investigated the effects of SG on gastric contractility[10]. The lack of studies focusing on the effects of SG on gastric contractility may be related to the high invasiveness and costs associated with the techniques used[11,12]. The alternating current biosusceptometry (ACB) is a low-cost and noninvasive technique extensively used for GI motility studies in humans and animals[13–18]. ACB enables a real-time assessment of GI transit (*e.g.*, gastric emptying, orocecal transit) and contractility

*Corresponding author at: Instituto de Biociências, UNESP – Rua Prof. Dr. Antonio Celso Wagner Zanin, 18618-689 Botucatu, Brazil.
E-mail address: mj.almeida@unesp.br (M.J.A. de Almeida).

https://doi.org/10.1016/j.soda.2025.100213
Received 3 December 2024; Accepted 11 April 2025
Available online 4 June 2025

parameters in the same measurement using magnetic tracers. Due to practical and ethical challenges on human subjects, animal models are essential for understanding the effects of SG on the GI tract. The impact of SG in rats' weight loss, food intake, and metabolic parameters have been extensively reported[19–21]; however, the relationship between gastric contractility and emptying associated with morphometry after SG still remain unclear. This study aimed to compare changes in metabolic parameters, GI motility and gastric morphology following SG in rats.

2. Materials and methods

2.1. Animals and experimental protocols

The Committee on Animal Research and Ethics approved all the experiments and procedures (CEUA Protocol number 1067) performed following the Ethical Principles in Animal Research adopted by the Brazilian College of Animal Experimentation (COBEA). The timeline for the experimental protocol is summarized in Fig. 1.

Thirty-two 45-day-old male *Wistar* rats were obtained from the ANILAB Laboratory (Paulínia, SP, Brazil) and maintained under controlled temperature (24 ± 2 °C), humidity (60 ± 5 %), and a 12 h light/dark cycle. During 12 consecutive weeks, from 45 days of life, sixteen rats, divided into Obese groups, were fed *ad libitum* on a high sugar-fat diet (HSF) containing 53.5 % carbohydrates, 18.0 % proteins, and 16.5 % fats, with an energy density of 4.35j kcal/g. The diet consisted of soybean meal, sorghum, soybean peel, dextrin, sucrose, fructose, lard, vitamins, and minerals. The diet protocol was developed at the São Paulo State University (UNESP), Medical School, Botucatu, Brazil, and was published previously[22]. For the Control groups, sixteen animals received a standard composed (SC) of soybean meal, sorghum, soybean peel, dextrin, soy oil, vitamins, and minerals, with caloric content of 3.59 kcal/g. At the end of the 12th week, the rats were assigned to four experimental groups: Control (n = 8, no intervention); Control sleeve gastrectomy SG (n = 8); Obese (n = 8, no intervention); and Obese sleeve gastrectomy SG (n = 8).

2.2. Surgical techniques

After 12-hour fasting, the rats were anesthetized with ketamine (30 mg/kg) and xylazine (15 mg/kg) injected intraperitoneally. Subcutaneous administration of enrofloxacin (5 mg/kg) and tramadol (10 mg/kg) were performed immediately before surgery. The animals received meloxicam (1 mg/kg) and tramadol (10 mg/kg) subcutaneously for three days as postoperative care. After surgery, the rats were fed a liquid diet (HSF diet mixed with water) for three days and then returned to the same diet as preoperatively[23].

2.2.1. Sleeve gastrectomy

SG was performed as previously described[23]. Briefly, after a midline abdominal incision of 1.5 cm from the xiphoid process down, the stomach was exteriorized, and a 7 FR catheter was passed through the mouth to the duodenum to standardize the size of the gastric sleeve. The stomach's fundus and greater curvature were removed with an electric scalpel while preserving the gastroesophageal junction and the pylorus. The stomach was then closed with a 4-0 polypropylene suture in two layers creating the gastric sleeve. The muscle layer's closure was performed using a 4-0 non-absorbable nylon suture and on the skin with 4-0 silk sutures.

2.3. Nutritional analysis

Body weight gain (g) and the average food consumption (g) were measured at 30th day for all the groups. The feed efficiency and energy intake were calculated as follows[24]:

$$Food\ efficiency\ (\%) = \frac{Body\ weight\ gain\ (g)}{Avarage\ energy\ intake\ (kcal/day)} \times 100 \quad (1)$$

$$Energy\ intake\ (kcal/day) = \frac{Average\ food\ consumption\ (g)}{Metabolizable\ energy\ of\ the\ diet\ (kcal)} \times 100 \quad (2)$$

2.4. Gastrointestinal motility measurements

The signal intensity obtained from an ACB measurement is directly proportional to the amount of magnetic material. The direct relation between the amount of magnetic material and signal intensity enables the evaluation of GI transit. Furthermore, the contraction of a stomach containing magnetic material increases the distance between the material and the sensor on the abdominal surface. At the same time, the relaxation of the segment decreases the distance, and therefore increases the signal registered by the ACB sensor. These signal modulations allow the assessment of contractile activity noninvasively using the ACB technique. Details on the instrumentation and working principles are described elsewhere[16,25,26].

GI motility measurements were performed preoperatively, and 30 days postoperatively, in all the groups. Gastric emptying, orocecal transit, and gastric contractility were recorded during the same day. Rats were fasted for 12 h and fed with a 2 g test meal of 0.5 g of magnetic tracers incorporated into 1.5 g of standard rat chow (Presence Nutrição Animal, Paulínia, SP, Brazil). Manganese ferrite ($MnFe_2O_4$) microparticles, with a size between 53 and 75 μm, were used as a non-absorbable and inert magnetic tracer at any GI pH[14].

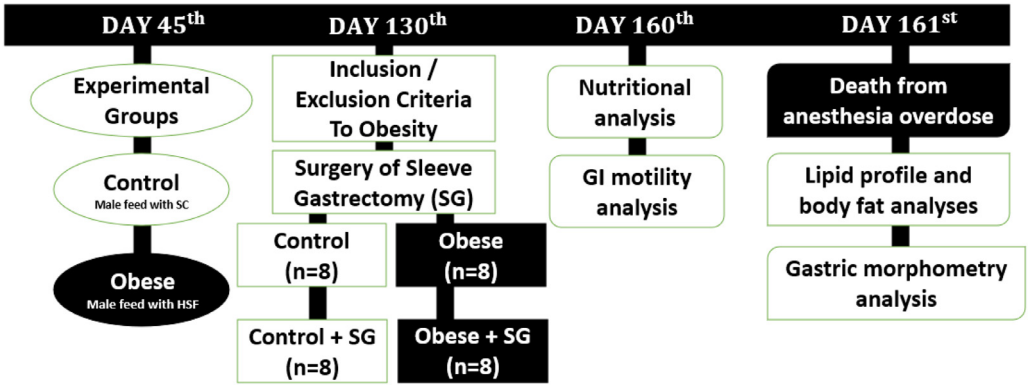

Fig. 1. Timeline of the experiment. Control (SC: standard composed), obese (HFS: high-sugar fat diet), control + SG and obese + SG (performed the procedure of sleeve gastrectomy surgery).

For gastric emptying and orocecal transit measurements, the ACB sensor was placed on the gastric and cecum projections (based on external anatomical references) to measure magnetic signal intensity. Subsequent measurements were performed at these two same points at regular 15 min intervals for 6 h[15].

Thirty minutes after beginning gastric emptying and orocecal transit measurements, the rats were anesthetized with isoflurane (4.0 % induction and 1.5 % maintenance) for the gastric contractility recordings. The rats were kept in a supine position, and the ACB sensor was positioned in the gastric projection for a 20 min signal recording[15]. The signal was acquired at a sampling rate of 20 Hz and digitized using an A/D board (MP100 System; BIOPAC Inc., Santa Barbara, CA, USA). After the gastric contractility recordings, the gastric emptying and orocecal transit measurements continued with the awake rats.

2.5. ACB data analysis

All raw signals were analyzed in MatLab (Mathworks Inc., Natick, USA).

Gastric emptying and orocecal transit time: Statistical moments were calculated through the temporal average pondered by magnetic intensity values normalized by the area under the curve[15,16,27]. The following parameters were quantified: mean gastric emptying time (MGET), which was defined as the time t (min) when a mean amount of magnetic tracer was emptied from the stomach; mean cecum arrival time (MCAT), defined as the time t (min) when an increase occurred in the mean amount of tracer in the cecum.

Gastric contractility: Firstly, the signal was filtered by a bi-directional Butterworth band-pass filter with a cut-off frequency of $1.0 - 9.0$ cycles per minute (cpm). Afterward, Fast Fourier transform (FFT) was used, and the highest peak of each FFT was considered the gastric dominant frequency, expressed as (cpm) and amplitude (dB). Gastric contractility signals were also visually analyzed regarding the waveform. Signal waveforms presenting a morphology of irregular peaks (*e. g.*, spikes) were classified as non-sinusoidal. Moreover, the amplitude (A) of gastric contractions was determined by computing the ratio between the intensity of the highest frequency peak (P) and the intensity of the noise peak (P') and expressed in decibels (dB) using the formula: $A = 10\log_{10}\frac{P}{P'}$[28]. The normal frequency range was the mean ± SD of the gastric dominant frequency obtained preoperatively[29,30].

2.6. Lipid profile and body fat analyses

On the 31st day after surgery, rats were killed by decapitation under deep anesthesia with ketamine. Blood samples were collected in non-additive tubes, and a laparotomy was performed to collect fat pads. The serum was separated by centrifugation at 1,490 g for 15 min at 4 °C and stored at -80 °C to assess serum parameters. Serum levels of total cholesterol (TC), triglycerides (TG), and high-density lipoproteins (HDL-C) were measured by the enzymatic methodology[31]. Values of very-low-density lipoprotein (VLDL-C) were estimated according to the calculation proposed by Knopfholz et al.[32].

Fat pads of adipose tissue were dissected, dipped in saline, and after the excess was removed, tissues were weighted. The total body fat was measured from the sum of the individual fat pad weights: visceral, retroperitoneal, and epididymal fat. The adiposity index (%) was calculated as follows[33]:

$$Adiposity\ index\ (\ \%) = \frac{Total\ body\ fat\ (g)}{Body\ weight\ (g)} \times 100 \quad (3)$$

2.7. Histological and gastric morphometry analysis

Tissue samples from the gastric body were fixed in 10 % neutral buffered formalin for 24 hours, dehydrated with serial alcohol and xylol solutions. Samples were included in paraffin, and histological cuts were performed with 4 μm thickness, stained with hematoxylin and eosin (HE). Images were acquired using an Eclipse E200-Nikon optical microscope (Nikon), in objective x10, equipped with a 5.0 MP digital camera system (model ISH 500, Opton), and connected to a computer with an image capture program (TCapture). All analyses were performed using ImageJ software (NIH). The morphometric analysis was carried out by measuring the gastric mucosa, muscularis mucosa, and submucosa thickness. Furthermore, histopathological examination was performed under light microscopy for graded assessment of leukocyte infiltration of all experimental groups, analyzed in a objective x40 (Table 1)[34,35].

2.8. Statistical analysis

All parameters were tested for normality using the Shapiro-Wilk test, and results were expressed as mean ± SD or median (interquartile range). A comparison of nutritional analysis, lipid profile, body fat, gastric morphometry, and histopathology among the groups was carried out by the unpaired Student's t-test (normal distribution) or Kruskal-Wallis test followed by Dunn's multiple comparisons test. The difference between GI parameters was determined by one-way analysis of variance (ANOVA) followed by the post hoc Tukey's test (normal distribution). Values of $p < 0.05$ were considered statistically significant. All statistical analyses were performed using GraphPad Prism 6 software (GraphPad Software, La Jolla, USA).

3. Results

3.1. Gastrointestinal motility

The MGET (Fig. 2A) exhibited a significant decrease on the 30th day in both control + SG group (79.3 ± 11.3 min, $p < 0.05$) and the obese group (113.9 ± 3.6 min, $p < 0.05$) in comparison to the control group (128.4 ± 7.8 min). Additionally, the obese + SG group (88.6 ± 8.4 min, $p < 0.05$) showed a significant decrease compared to the obese group (113.9 ± 3.6 min). The MCAT decreased from (259.6 ± 16.1 min) in the obese group to (230.0 ± 17.6 min, $p < 0.05$) in the obese + SG group (as shown in Fig. 2B).

The gastric dominant frequency on the 30th day, in the obese + SG group (3.5 ± 0.4 cpm) were significantly decreased, as shows (Fig. 3A), compared to the obese group (4.5 ± 0.3 cpm, $p < 0.05$). The amplitude of gastric contractions was significantly lower in the control + SG group (10.8 ± 3.6 dB, $p < 0.05$) compared to obese + SG group (15.8 ± 2.7 dB) (Fig. 3B).

3.2. Nutritional analysis

Fig. 4 shows nutritional analysis. Fig. 4A shows the average body weight gain, control rats increased by 5.12 % ± 25.3 %. In the control rats subjected to SG, the weight gain was lower (1.39 % ± 22.1 %). In the obese rats, the weight gain was more pronounced, with an average increase of (7.01 % ± 45.1 %). However, in the obese rats that underwent SG, there was a significant reduction in body weight (12.65 % ± 63.7 %), this marked variation in the standard deviation may reflect individual responses to the surgical intervention. Fig. 4B show that the

Table 1
Histopathological scoring criteria. HPF: high power field.

Pathological state	Score	
Leukocyte infiltration	0	Absent
	1	2-10/HPF
	2	11-20/HPF
	3	21-30/HPF
	4	>31/HPF

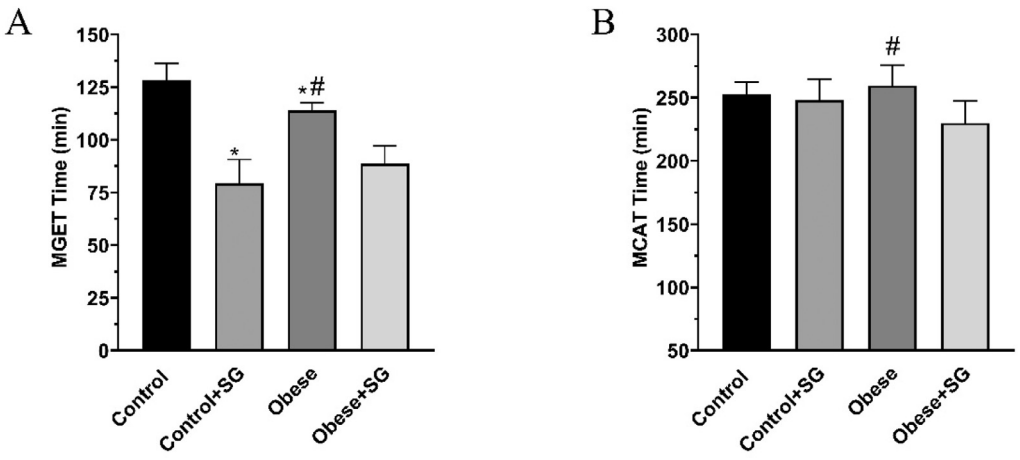

Fig. 2. Gastric emptying and orocecal transit results before and after SG in rats. **(A)** Mean gastric emptying time (MGET) and **(B)** Mean cecum arrival time (MCAT) at 30 days after surgery. Data are presented as mean ± SD. *p < 0.05 vs Control; #p < 0.05 vs Obese + SG (ANOVA followed by the Tukey multiple comparison test).

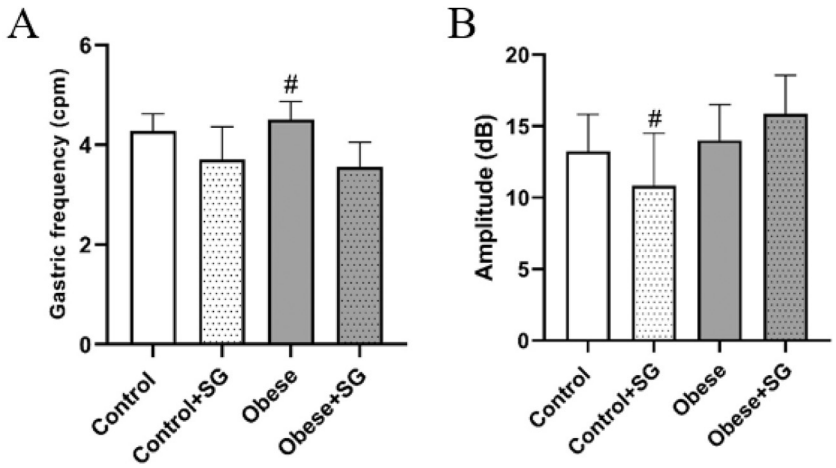

Fig. 3. Gastric contractility parameters 30 days after SG. **(A)** Gastric dominant frequency and **(B)** amplitude (dB). Obese Data analyzed ANOVA followed by Tukey and expressed as mean ± SD. *p < 0.05 vs Control; #p < 0.05 vs Obese + SG.

adiposity index was significantly higher in the obese group (4.94 % ± 1.87 %) compared to the control group (2.36 % ± 0.4 %, p<0.05), confirming the accumulation of adipose tissue under obesity conditions. Importantly, the obese group subjected to SG showed a significant reduction in the adiposity index (2.89 % ± 0.94 %, p<0.01). There was no significant difference in energy intake among the groups, indicating that the observed variations in body weight and adiposity index cannot be attributed to differences in caloric intake, as shown in Fig. 3C.

3.3. Lipid profile and body fat analyses

Serum levels of lipids and body fat results are shown in Table 2. The control group (2.89 % ± 9.7) had significantly higher total cholesterol levels compared to the control + SG group (46.2 ± 12.1, *p < 0.05). In the obese group (57.7 ± 12.5), total cholesterol did not differ significantly from the control. After SG, the obese + SG group also showed a slight reduction in total cholesterol levels (49.2 ± 12.6), but without statistical significance compared to the control.

Triglyceride levels were significantly higher in the obese group (71.6 ± 29.9) compared to the control group (*p<0.05), which is consistent with literature associating obesity with increased triglycerides. After SG, triglyceride levels decreased in the obese + SG group (46.2 ± 12.7), although they did not return to control group levels, indicating significant improvement after surgery.

The obese group showed an increase in VLDL levels (16.0 ± 5.4) compared to the control group (7.1 ± 1.9), reflecting the increase in triglycerides. SG have normalized VLDL levels, with values close to the control in the control + SG (9.0±2.0) and obese + SG (9.2 ± 2.5) groups.

Obesity resulted in a significant reduction in HDL-C levels in the obese group (29.0 ± 3.3, *p<0.05) compared to the control group (49.6 ± 4.7). SG did not manage to restore HDL-C levels in the control + SG (32.7 ± 9.4) and obese + SG (28.6 ± 3.8) groups.

Non-HDL-C levels were higher in the obese group (28.7 ± 10.3) compared to the control group (18.7 ± 8.4), which is expected given the increase in LDL and VLDL associated with obesity. After SG, there was a reduction in the obese + SG group (24.2 ± 7.0), although not significant.

3.4. Histopathological and gastric morphometry analysis

The stomach's fundus and greater curvature were removed in SG, we observed post-mortem dilatation in all stomach regions. Gastric histopathological and morphometric analyses are presented in Figs. 5 and 6, respectively. The stomachs of the control and obese groups (Fig. 5A and C) showed a typical histological structure of the gastric muscular layer, whereas in both the control + SG and obese + SG groups (Fig. 5B and D), we observed a decrease in the thickness of the gastric muscular layer.

The thickness of the gastric mucosa was significantly decreased in both SG-treated groups, as shown in Fig. 6A. This reduction was particularly pronounced in the obese + SG group, highlighting the impact of sleeve gastrectomy on this gastric layer. In contrast, tissue remodeling was observed in the SG rats (Fig. 6C), showing multiple areas of

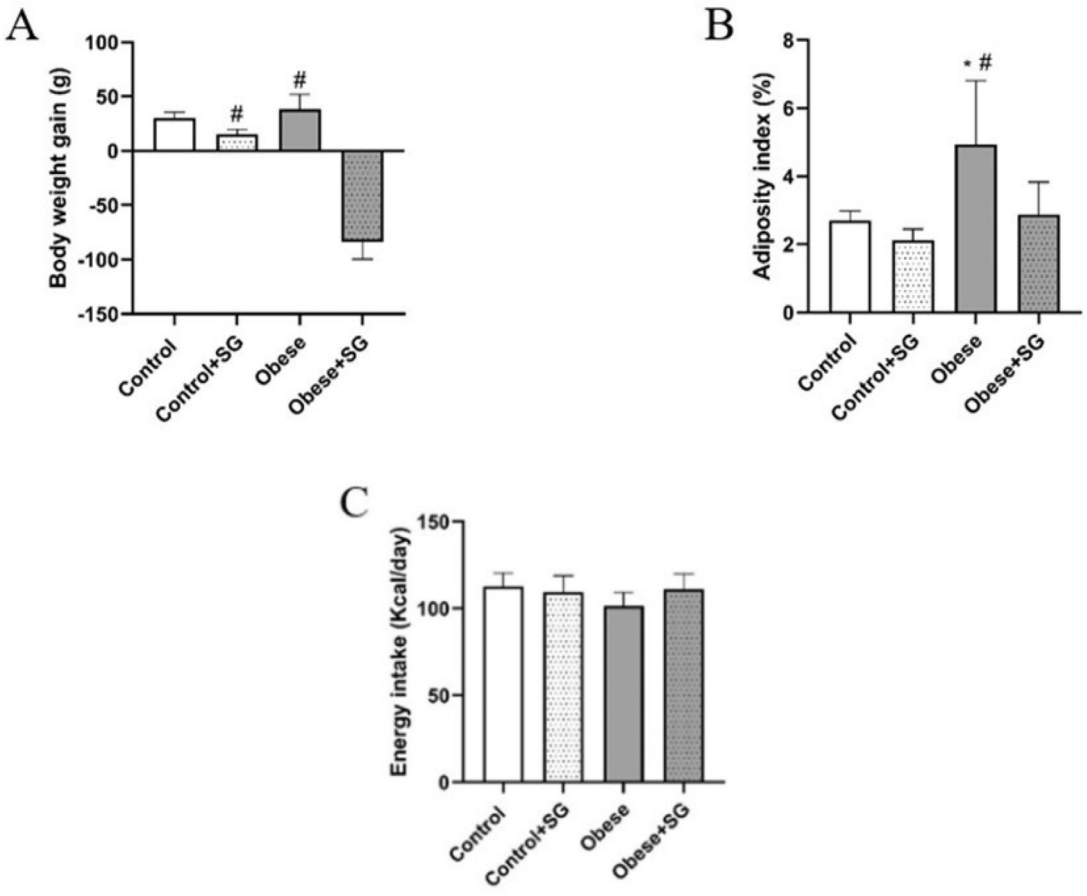

Fig. 4. Nutritional analysis. **(A)** Body weight gain (g) over 30 days, **(B)** Adiposity index (%) measured at the final of experiment, **(C)** Energy intake (kcal/day) **(D)** Food efficiency (%) were determined by the mean of 30 days. Experimental groups: control (n = 8), control + SG (n = 8), obese (n = 8) and obese + SG (n = 8). Data analyzed by ANOVA followed by Tukey and expressed as mean ± SD. *p < 0.05 vs Control; #p < 0.01 vs Obese + SG.

Table 2
Serum levels of lipids and adiposity index of control (n = 8), obese (n = 8), control + SG (n = 8), obese + SG (n = 8) groups. Data analyzed by ANOVA followed by Tukey test and are presented as mean ± SD, *p<0.05 vs Control.

	Control	Control SG	Obese	Obese SG
Total cholesterol	67.5±9.7	46.2±12.1*	57.7±12.5	49.2±12.6
Triglycerides	35.5±9.3	45.2±10.3	71.6±29.9*	46.2±12.7
VLDL	7.1±1.9	9.0±2.0	16.0±5.4	9.2±2.5
HDL-C	49.6±4.7	32.7±9.4*	29.0±3.3*	28.6±3.8
Non-HDL-C	18.7±8.4	13.5±5.3	28.7±10.3	24.2±7.0

leukocyte infiltration in the muscularis mucosa, submucosal, and mucosal layers of the gastric body (Fig. 6D). Gastric tissue alterations were further quantified using a pathological score (Fig. 6D), which revealed significantly higher leukocyte infiltration in both SG groups compared to the control and obese groups ($p < 0.05$). This indicates a notable inflammatory response in the gastric tissue following SG. Inflammatory cell infiltration was observed in all layers—muscularis, submucosa, and mucosa—30 days post-SG.in the gastric tissue following SG. Inflammatory cell infiltration was observed in all layers—muscularis, submucosa, and mucosa—after 30 days post-SG.

4. Discussion

Our study Our study reported significant alterations in gastric emptying, orocecal transit time, gastric mechanical activity, and gastric morphometry after sleeve gastrectomy (SG). At the end of the experimental period, while the body weight of the rats increased as expected, the SG group exhibited significantly lower body weight gain compared to the control group. An unexpected increase in baseline caloric intake was observed by the end of the experimental protocol. This paradoxical increase may be associated with the loss of restrictive gastric capacity due to gastric enlargement or dilation, as observed post-mortem in both SG groups, similar to findings by Guimarães et al.[19]. Gastric sleeve dilation has been noted in humans as well, though it does not always compromise the procedure's success in achieving weight loss[36]. The lack of reduced caloric intake despite weight loss in SG rats could also be attributed to accelerated gastrointestinal (GI) transit or nutrient malabsorption, a phenomenon also reported in human studies[37].

Before surgery, the gastric emptying curve was characterized by meal retention, reflecting the accommodation reflex. After SG, the profile

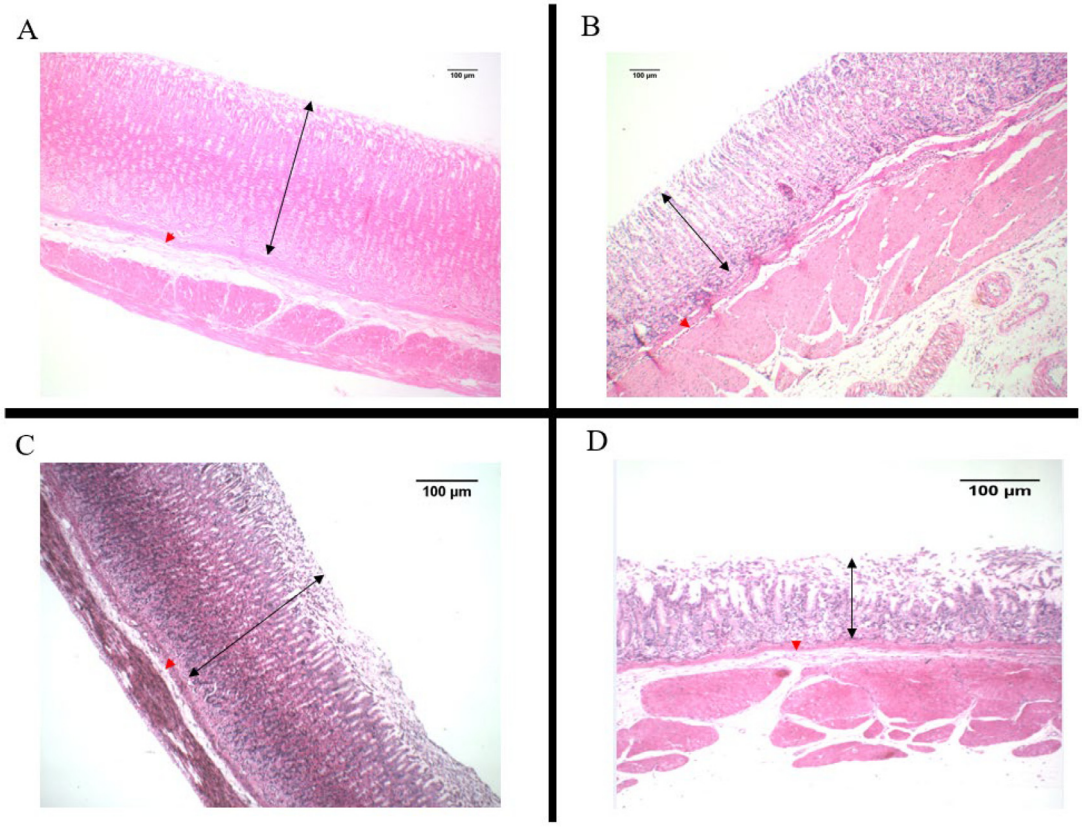

Fig. 5. Effect of SG on gastric body samples. Histological photomicrographs using HE stain of **(A)** control, **(B)** control + SG **(C)** obese **(D)** obese + SG (× 10 objective) (red arrow: muscularis mucosa layer/black arrow: mucosa layer).

changed to an exponential decay, lacking the accommodation reflex. Consequently, the Mean Gastric Emptying Time (MGET) was significantly accelerated 30 days post-SG, consistent with Chambers et al.[20], who also reported accelerated gastric emptying in a rodent SG model via scintigraphy. This acceleration was linked to impaired inhibitory feedback from the intestine and increased intragastric pressure. The removal of the fundus, responsible for the accommodation reflex and controlling gastric pressure, likely promoted this increase in pressure and, subsequently, faster gastric emptying[8,38]. While our study did not assess intragastric pressure or intestinal feedback, the observed alterations in gastric contractility and tissue remodeling, such as changes in the muscular layer, likely contributed to the acceleration.

Preoperative gastric contractility signals presented expected stationary, sinusoidal waveforms within a narrow frequency range, as noted in earlier studies[15,39]. Post-SG, however, the contractility signals were marked by irregular peaks, frequency drifts, and bradygastria. These changes suggest an impaired ability of the stomach muscles to contract properly following the excision of the greater curvature. This erratic gastric contractility persisted even 30 days after SG, implying that further studies are necessary to determine whether these alterations may be long-lasting.

Gastric contractility originates from gastric slow waves generated by electrical activity in the interstitial cells of Cajal (ICCs)[40,41]. The highest slow-wave frequency, typically located in the greater curvature, controls the stomach's dominant frequency[42–45]. Previous rodent studies have demonstrated that severing the antrum from the corpus results in a significant reduction in antral slow-wave frequency[45]. In a proximal gastrectomy rat model, excision of the upper corpus led to bradygastria[15]. In our study, SG's removal of the greater curvature likely disrupted the ICC network, resulting in a decreased gastric dominant frequency and severe alterations in the contractility waveform. To our knowledge, no other rodent studies have focused on gastric contractility post-SG. In humans, SG increases slow-wave propagation velocity and antral propulsion, though no changes in dominant frequency have been reported[11,12].

Our morphometric analysis revealed significant remodeling of the gastric muscular layer post-SG. The thickness of both the mucosa and muscularis mucosa layers was reduced compared to sham rats. Additionally, leukocyte infiltration in multiple gastric layers, including the muscularis, submucosa, and mucosa, indicates post-SG inflammation, which has been previously documented[46,47]. Inflammation can significantly impact smooth muscle function, influencing gastric contractility by affecting ion channels, signaling pathways, or transcription factors[48]. In the small intestine, inflammation has been associated with disruptions in the ICC network, leading to uncoupling between ICCs and smooth muscle cells and impaired contractility[49]. Our findings of decreased dominant frequency and altered waveforms post-SG may result from such inflammatory processes.

Beyond the stomach, SG may also induce motility alterations in the broader GI tract. Our results show that while orocecal transit curve patterns remained consistent before and after SG, the magnetic tracer reached the cecum faster post-SG, indicating a shortened Mean Cecum Arrival Time (MCAT). Accelerated intestinal transit has also been observed in both rodent and human SG models[20,50,51], potentially independent of faster gastric emptying. The quicker arrival of nutrients into the distal intestine, resulting from accelerated gastric emptying and intestinal transit, has been proposed as a mechanism for improved glucose homeostasis and increased glucagon-like peptide-1 (GLP-1) release post-SG[20,51–53].

In rats, techniques such as phenol red recovery are considered the gold standard for assessing GI transit, though they require animal sacrifice, necessitating large sample sizes[54–56]. Other methods, such as scintigraphy, ^{13}C breath tests, and radiopaque tracers, have their limitations, including radiation exposure and high cost [57,58]. Current techniques for evaluating gastric contractility in rats are limited, with manometry being highly invasive and magnetic

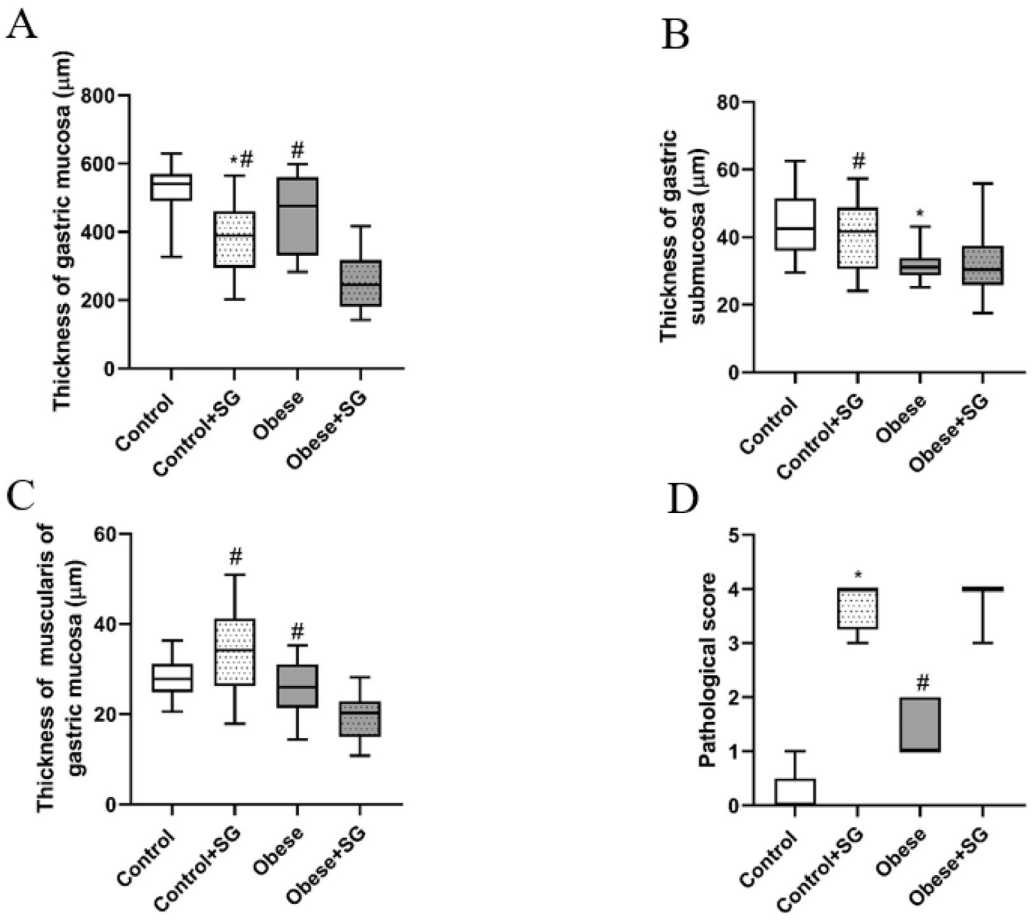

Fig. 6. Gastric morphometry analysis of: **(A)** morphometrical gastric mucosa, **(B)** morphometrical gastric submucosa **(C)** and muscularis of gastric mucosa. In **(D)** pathological score. Data analyzed by Kruskal-Wallis test followed by Dunn's multiple comparisons test and expressed as median ± range, *p<0.05 vs Control; #p<0.05 vs Obese + SG.

resonance imaging complex[57,59]. In contrast, alternating current biosusceptometry (ACB) offers a non-invasive, low-cost alternative for assessing GI motility. ACB provides the advantage of measuring multiple GI parameters simultaneously, reducing the need for multi-instrumental approaches.

5. Conclusion

In summary, this study demonstrates alterations in metabolic parameters, GI motility, and gastric morphology in rats post-SG. Both MGET and MCAT were accelerated, potentially due to increased intragastric pressure. SG-induced excision of the greater curvature led to bradygastria and altered gastric contractility signals. Significant gastric tissue remodeling and inflammation were also observed, likely affecting contractile activity. These dysmotilities persisted throughout the 30-day observation period, indicating the need for extended follow-up studies to determine if these effects are permanent. Therefore, non-invasive, reproducible approaches, such as ACB, are desirable for long-term monitoring of SG outcomes in animal models.

Disclosure

All the authors declare that there are no conflicts of interest.

Declaration of competing interest

The authors declare that they have no known competing financial interests or personal relationships that could have appeared to influence the work reported in this paper.

CRediT authorship contribution statement

Gustavo Serafim Rodrigues: Data curation, Writing – review & editing. **Leonardo Antônio Pinto:** Data curation, Formal analysis, Investigation, Software, Writing – original draft. **Erick Guilherme Stoppa:** Data curation, Formal analysis, Resources, Writing – review & editing. **Mariana Pirani Rocha Machado:** Conceptualization, Data curation, Investigation, Resources, Writing – original draft. **Loyane Almeida Gama:** Conceptualization, Data curation, Investigation, Methodology, Resources, Writing – original draft. **Guilherme Augusto Soares:** Data curation, Formal analysis, Methodology, Resources, Supervision, Validation, Writing – review & editing. **Rozemeire Garcia Marques:** Supervision, Validation, Writing – original draft. **Madileine Francely Américo:** Conceptualization, Data curation, Formal analysis, Investigation, Resources, Supervision, Validation, Writing – original draft, Writing – review & editing. **José Ricardo de Arruda Miranda:** Conceptualization, Data curation, Formal analysis, Funding acquisition, Methodology, Project administration, Supervision, Writing – original draft, Writing – review & editing.

Acknowledgments

This work was supported by the São Paulo Research Foundation (FAPESP - grant no. 2015/14923-9), the National Council for Scientific and Technological Development (CNPq), and the Coordination for the Improvement of Higher Education Personnel (CAPES – Finance code 001). We would like to thank the São Paulo State University Medical School for the technical support with the surgical procedures and diets.

References

[1] Must A, Spadano J, Coakley EH, Field AE, Colditz G, Dietz WH. The disease burden associated with overweight and obesity. JAMA 1999;282:1523–9.
[2] Bray GA, Tartaglia LA. Medicinal strategies in the treatment of obesity. Nature 2000;404:672–7.
[3] Buchwald H, Avidor Y, Braunwald E, et al. Bariatric surgery: a systematic review and meta-analysis. JAMA 2004;292:1724–37.
[4] Diamantis T, Apostolou KG, Alexandrou A, Griniatsos J, Felekouras E, Tsigris C. Review of long-term weight loss results after laparoscopic sleeve gastrectomy. Surg Obesity Related Diseases: Official J Am Society Bariatric Surg 2014;10:177–83.
[5] Angrisani L, Santonicola A, Iovino P, Formisano G, Buchwald H, Scopinaro N. Bariatric Surgery worldwide 2013. Obes Surg 2015;25:1822–32.
[6] Quercia I, Dutia R, Kotler DP, Belsley S, Laferrere B. Gastrointestinal changes after bariatric surgery. Diabetes Metab 2014;40:87–94.
[7] Won KJ, Sanders KM, Ward SM. Interstitial cells of Cajal mediate mechanosensitive responses in the stomach. Proc Natl Acad Sci U S A 2005;102:14913–8.
[8] Yehoshua RT, Eidelman LA, Stein M, et al. Laparoscopic sleeve gastrectomy—volume and pressure assessment. Obes Surg 2008;18:1083–8.
[9] Hansen MB. Neurohumoral control of gastrointestinal motility. Physiol Res 2003;52:1–30.
[10] Sioka E, Tzovaras G, Perivoliotis K, et al. Impact of laparoscopic sleeve gastrectomy on gastrointestinal motility. Gastroenterol Res Pract 2018;2018:4135813.
[11] Berry R, Cheng LK, Du P, et al. Patterns of abnormal gastric pacemaking after sleeve gastrectomy defined by laparoscopic high-resolution electrical mapping. Obes Surg 2017;27:1929–37.
[12] Baumann T, Kuesters S, Grueneberger J, et al. Time-resolved MRI after ingestion of liquids reveals motility changes after laparoscopic sleeve gastrectomy—preliminary results. Obes Surg 2011;21:95–101.
[13] Miranda JR, Oliveira RB, Sousa PL, Braga FJ, Baffa O. A novel biomagnetic method to study gastric antral contractions. Phys Med Biol 1997;42:1791–9.
[14] Americo MF, Marques RG, Zandona EA, et al. Validation of ACB in vitro and in vivo as a biomagnetic method for measuring stomach contraction. Neurogastroenterol Motility Official J Europ Gastrointest Motility Society 2010;22(1340-1344):e1374.
[15] Calabresi MF, Quini CC, Matos JF, et al. Alternate current biosusceptometry for the assessment of gastric motility after proximal gastrectomy in rats: a feasibility study. Neurogastroenterol Motility Official J Europ Gastrointest Motility Society 2015;27:1613–20.
[16] Quini CC, Americo MF, Cora LA, et al. Employment of a noninvasive magnetic method for evaluation of gastrointestinal transit in rats. J Biol Eng 2012;6:6.
[17] Prospero AG, Pinto LA, Matos RVR, et al. New device for active gastric mechanical stimulation. Neurogastroenterol Motility Official J Europ Gastrointest Motility Society 2021:e14169.
[18] Pinto L, Soares G, Prospero A, et al. An easy and low-cost biomagnetic methodology to study regional gastrointestinal transit in rats. Biomedizinische Technik Biomed Eng 2021.
[19] Guimaraes M, Nora M, Ferreira T, et al. Sleeve gastrectomy and gastric plication in the rat result in weight loss with different endocrine profiles. Obes Surg 2013;23:710–7.
[20] Chambers AP, Smith EP, Begg DP, et al. Regulation of gastric emptying rate and its role in nutrient-induced GLP-1 secretion in rats after vertical sleeve gastrectomy. Am J Physiol Endocrinol Metabol 2014;306:E424–32.
[21] Cabrera A, Vives M, Molina A, et al. Gastric plication and sleeve gastrectomy in an experimental model of obesity: new insights into weight loss, intake and metabolic results. Obes Surg 2018;28:3259–67.
[22] Francisqueti FV, Minatel IO, Ferron AJT, et al. Effect of gamma-oryzanol as therapeutic agent to prevent cardiorenal metabolic syndrome in animals submitted to high sugar-fat diet. Nutrients 2017;9.
[23] Bruinsma BG, Uygun K, Yarmush ML, Saeidi N. Surgical models of Roux-en-Y gastric bypass surgery and sleeve gastrectomy in rats and mice. Nat Protoc 2015;10:495–507.
[24] Diniz YS, Faine LA, Galhardi CM, et al. Monosodium glutamate in standard and high-fiber diets: metabolic syndrome and oxidative stress in rats. Nutrition 2005;21:749–55.
[25] Baffa O, Oliveira RB, Miranda JR, Troncon LE. Analysis and development of AC biosusceptometer for orocaecal transit time measurements. Med Biol Eng Comput 1995;33:353–7.
[26] Cora LA, Romeiro FG, Stelzer M, et al. AC biosusceptometry in the study of drug delivery. Adv Drug Deliv Rev 2005;57:1223–41.
[27] Podczeck F, Newton JM, Yuen KH. The description of the gastrointestinal transit of pellets assessed by gamma scintigraphy using statistical moments. Pharm Res 1995;12:376–9.
[28] Gama LA, Rocha Machado MP, Beckmann APS, Miranda JRA, Corá LA, Américo MF. Gastrointestinal motility and morphology in mice: strain-dependent differences. Neurogastroenterol Motil 2020;32(6):e13824.
[29] Cucchiara S, Franzese A, Salvia G, et al. Gastric emptying delay and gastric electrical derangement in IDDM. Diabetes Care 1998;21:438–43.
[30] Long QL, Fang DC, Shi HT, Luo YH. Gastro-electric dysrhythm and lack of gastric interstitial cells of cajal. World J Gastroenterol 2004;10:1227–30.
[31] Friedman RB, Anderson RE, Entine SM, Hirshberg SB. Effects of diseases on clinical laboratory tests. Clin Chem 1980;26:1D–476D.
[32] Knopfholz J, Disserol CC, Pierin AJ, et al. Validation of the friedewald formula in patients with metabolic syndrome. Cholesterol 2014:261878 2014.
[33] Leopoldo AS, Lima-Leopoldo AP, Sugizaki MM, et al. Involvement of L-type calcium channel and SERCA2a in myocardial dysfunction induced by obesity. J Cell Physiol 2011;226:2934–42.
[34] Shahin NN, Abdelkader NF, Safar MM. A novel role of Irbesartan in gastroprotection against indomethacin-induced gastric injury in rats: targeting DDAH/ADMA and EGFR/ERK signaling. Sci Rep 2018;8:4280.
[35] Liu J, Wang F, Luo H, et al. Protective effect of butyrate against ethanol-induced gastric ulcers in mice by promoting the anti-inflammatory, anti-oxidant and mucosal defense mechanisms. Int Immunopharmacol 2016;30:179–87.
[36] Disse E, Pasquer A, Pelascini E, et al. Dilatation of sleeve gastrectomy: myth or reality? Obes Surg 2017;27:30–7.
[37] Pech N, Meyer F, Lippert H, Manger T, Stroh C. Complications and nutrient deficiencies two years after sleeve gastrectomy. BMC Surg 2012;12:13.
[38] Indireshkumar K, Brasseur JG, Faas H, et al. Relative contributions of "pressure pump" and "peristaltic pump" to gastric emptying. Am J Physiol Gastrointest liver Physiol 2000;278:G604–16.
[39] Marques RG, Americo MF, Spadella CT, Cora LA, Oliveira RB, Miranda JR. Different patterns between mechanical and electrical activities: an approach to investigate gastric motility in a model of long-term diabetic rats. Physiol Meas 2014;35:69–81.
[40] Hirst GD, Ward SM. Interstitial cells: involvement in rhythmicity and neural control of gut smooth muscle. J Physiol 2003;550:337–46.
[41] Sanders KM. A case for interstitial cells of Cajal as pacemakers and mediators of neurotransmission in the gastrointestinal tract. Gastroenterology 1996;111:492–515.
[42] Kelly KA, Code CF. Canine gastric pacemaker. Am J Physiol 1971;220:112–8.
[43] Chen JD, Zou X, Lin X, Ouyang S, Liang J. Detection of gastric slow wave propagation from the cutaneous electrogastrogram. Am J Physiol 1999;277:G424–30.
[44] Hashitani H, Garcia-Londono AP, Hirst GD, Edwards FR. Atypical slow waves generated in gastric corpus provide dominant pacemaker activity in guinea pig stomach. J Physiol 2005;569:459–65.
[45] Ordog T, Baldo M, Danko R, Sanders KM. Plasticity of electrical pacemaking by interstitial cells of cajal and gastric dysrhythmias in W/W mutant mice. Gastroenterology 2002;123:2028–40.
[46] Mahmoud YI, Abd El-Ghffar EA. Spirulina ameliorates aspirin-induced gastric ulcer in albino mice by alleviating oxidative stress and inflammation. Biomed Pharmacother 2019;109:314–21.
[47] Sagun K, Roy VK, Kumar RS, et al. Antioxidant potential, anti-inflammatory activity and gastroprotective mechanisms of Mallotus roxburghianus (Muell.) against ethanol-induced gastric ulcers in Wistar albino rats. J Funct Foods 2017;36:448–58.
[48] Shea-Donohue T, Notari L, Sun R, Zhao A. Mechanisms of smooth muscle responses to inflammation. Neurogastroenterol Motility Official J Europ Gastrointest Motility Society 2012;24:802–11.
[49] Der T, Bercik P, Donnelly G, et al. Interstitial cells of cajal and inflammation-induced motor dysfunction in the mouse small intestine. Gastroenterology 2000;119:1590–9.
[50] Melissas J, Leventi A, Klinaki I, et al. Alterations of global gastrointestinal motility after sleeve gastrectomy: a prospective study. Ann Surg 2013;258:976–82.
[51] Shah S, Shah P, Todkar J, Gagner M, Sonar S, Solav S. Prospective controlled study of effect of laparoscopic sleeve gastrectomy on small bowel transit time and gastric emptying half-time in morbidly obese patients with type 2 diabetes mellitus. Surg obesity Related Diseases: Official j Am Society Bariatric Surg 2010;6:152–7.
[52] Masuda T, Ohta M, Hirashita T, et al. A comparative study of gastric banding and sleeve gastrectomy in an obese diabetic rat model. Obes Surg 2011;21:1774–80.
[53] Sista F, Abruzzese V, Clementi M, Carandina S, Cecilia M, Amicucci G. The effect of sleeve gastrectomy on GLP-1 secretion and gastric emptying: a prospective study. Surg Obesity Related Diseases: Official J Am Society Bariatric Surg 2017;13:7–14.
[54] Bennink RJ, de Jonge WJ, Symonds EL, et al. Validation of gastric-emptying scintigraphy of solids and liquids in mice using dedicated animal pinhole scintigraphy. J Nuclear Med 2003;44:1099.
[55] Souza MAN, Souza MHLP, Palheta RC, et al. Evaluation of gastrointestinal motility in awake rats: a learning exercise for undergraduate biomedical students. Adv Physiol Educ 2009;33:343–8.
[56] Gondim FA, Rodrigues CL, da Graça JR, et al. Neural mechanisms involved in the delay of gastric emptying and gastrointestinal transit of liquid after thoracic spinal cord transection in awake rats. Autonom Neurosci Basic Clin 2001;87:52–8.
[57] Szarka LA, Camilleri M. Methods for measurement of gastric motility. AmPhysiol Gastrointest Liver Physiol 2009;296:G461–75.
[58] Camilleri M, Hasler WL, Parkman HP, Quigley EM, Soffer E. Measurement of gastrointestinal motility in the GI laboratory. Gastroenterology 1998;115:747–62.
[59] Lu KH, Cao J, Oleson ST, Powley TL, Liu Z. Contrast-enhanced magnetic resonance imaging of gastric emptying and motility in rats. IEEE Trans Biomed Eng 2017;64:2546–54.